Journal of Atmospheric and Terrestrial Physics, Vol. 41, pp. 1205–1221
Pergamon Press Ltd. 1979. Printed in Northern Ireland

Seasonal mean structure of the night-time *F2* region over Arecibo

S. FUKAO, T. SATO and I. KIMURA
Department of Electrical Engineering, Kyoto University, Kyoto, Japan

and

R. M. HARPER
Ionosphere Research Laboratory, Kyoto University, Uji, Japan

(*Received* 28 *November* 1978; *in revised form* 9 *May* 1979)

Abstract—Seasonal mean night-time variations of ion and electron temperatures, electron density, ion drift velocity, and light ion composition of the *F2* region are derived from incoherent scatter observations at Arecibo based on 19 nights of observation over the latest sunspot minimum years 1974–1976. It is shown that the downward flux of ionization is sufficient to maintain the nocturnal *F2* region against recombination at low latitudes. The difference in the electron density decay rate from summer to winter is consistent with the seasonal variation in magnitude of the ionization flux. The mean eastward electric field, which is responsible for any vertical component perpendicular to **B**, is very small throughout the night. However, the southward electric field, i.e. east–west ion drifts, shows a substantial systematic variation during the night, being southward (eastward ion drifts) before midnight and northward after midnight, with a mean amplitude of 1–2 mV m^{-1}. The H^+ ion concentration shows a marked seasonal variation. The mean relative concentration of H^+ ion to electron density at 500 km sometimes exceeds 50% before sunrise in winter. A strong anti-correlation of H^+ ion concentration with magnetic activity is observed. The observed ion temperatures average about 20–30 K higher than the prediction of the JACCHIA (1971) neutral model for the observed range of the 10.7 cm solar flux.

1. INTRODUCTION

There are several synoptic studies of the night-time *F2* region at Arecibo, Puerto Rico (18.3°N, 66.75°W). MOORCROFT (1969) and PRASAD (1968) obtained the night-time and seasonal variations of the ionic composition and temperature from the analysis of incoherent scatter spectra gathered near the sunspot minimum years of solar cycle 20 (1965–1967). The works of HO and MOORCROFT (1971, 1975, 1977) are concerned with data from the same period, while HAGEN and HSU (1974) discussed the vertical drift velocities along with other ionospheric parameters during the decaying period of the solar activity (February 1972). The analysis which follows is based on 19 nights of Arecibo data obtained during the latest sunspot minimum years 1974–1976. First we define the mean night-time variations of the ionospheric basic parameters for different seasons, including ion drift velocities as well as electron density, ion and electron temperatures, the altitude of the *F2* region and light ion concentrations.

Then we discuss the observed characteristics, especially the strong anti-correlation of light ion concentration with magnetic activity and the interrelation between the observed temperature and the exospheric temperature parameter of the JACCHIA 1971 model.

Finally the maintenance of the night-time ionosphere is discussed in connection with the question of the vertical flux of ionization. The present analysis confirms the results of HAGEN and HSU (1974) that the observed flux very closely matches the loss of ionization due to recombination. The difference in the electron density decay rate from summer to winter will be shown to be consistent with the seasonal variation in the ionization flux.

2. OBSERVATION AND ANALYSIS

2.1 *Observational technique*

The measurements are made by transmitting two different pulse schemes:

(1) Complex auto-correlation functions (ACFs) are measured by a single 296 μs pulse with altitude resolution of 45 km. The technique is essentially the same as that used by BEHNKE and HARPER (1973). The ACFs are calculated for a total of 11

altitudes spaced at 29 km intervals over the 200–500 km region. Eleven time delays (including the zero delay) are calculated with a spacing of 16 μs, giving a maximum time delay of 160 μs. Seventy per cent of the observation time is spent on this pulse scheme.

(2) A single 24 μs pulse is used to measure a power profile with a 3.5 km altitude resolution. The echo power is observed at 120 altitude levels with a 1.2 km spacing over the 80–156 km region and a 5.8 km spacing over the 156–457 km region. Thirty per cent of the observation time is used in order to measure accurately electron density profiles in the $F1$ region valley.

The Arecibo antenna must be pointed in at least three directions in order to measure the ion drift velocity vector. The antenna is tilted 15° from the zenith and alternately directed at 180°, 270° and 360° azimuth (measured clockwise from the north). At any given position the 296 μs pulse is transmitted for about 10 min. The antenna is then rotated to the next position, during which time (about 5 min) the 24 μs pulse is transmitted.

Line-of-sight velocities are determined by a least squares fit to a change in the phase of the complex ACF with time delay. All those velocity data are analyzed for simplicity under the assumption that the phase shift of the ACF is linearly proportional to time delay, i.e. that the entire plasma is assumed to move with a single velocity. The present analysis is not ideal, as the relative velocity between O^+ and H^+ ions appears to be large during periods of rapid temperature change in the O^+/H^+ transition region (VICKREY *et al.*, 1976). The line-of-sight velocities at the three positions are interpolated in time and combined to give the ion drift velocity vector. There is a systematic offset in the line-of-sight velocities due to a transmitter frequency change during the transmitted pulse. This offset affects the vertical velocity but not the horizontal velocity components, since the offsets cancel in transformation of the measured line-of-sight velocities into the velocity vector (HARPER *et al.*, 1976). It was not possible to measure the offset during each observation, and all the data were corrected for a fixed offset. This can introduce a systematic uncertainty of the order of 5 m s^{-1} in the vertical velocity component. The random error in the inferred velocity components is small when the ionosphere is uniform over scales of several hundred km, but it may be large when slab instabilities are present (BEHNKE, 1979). However, our use of highly averaged data should reduce the errors that may be present on individual nights.

2.2. *ACF analysis*

The experimental ACFs are matched with theoretically generated ACFs in a least-mean-squares sense. The present procedure is a direct descendant of that employed by WALDTEUFEL (1971) at Arecibo. The ions at the lowest altitude (~200 km) are assumed to be pure O^+, so that the ion and electron temperatures can be inferred from the first zero crossing and the depth of the first minimum of the ACF. This assumption may cause another error in derivation of ionospheric parameters below about 250 km, where the presence of the molecular ions such as O_2^+ and NO^+ is not negligible (e.g. WAND and PERKINS, 1970). The final values obtained by the least-mean-squares fitting procedure at this lowest altitude then become the starting point for the fitting at the next altitude, and so on.

It is assumed that the ion species present in the 200–500 km region are O^+, He^+ and H^+ ions. The theoretical ACFs are functions of ion mass, ion temperature T_i, electron temperature T_e, and electron density N_e. The electron density N_e is not important except when the Debye length D is greater than about 0.01λ, where λ is the radar wavelength (e.g. EVANS, 1969). For the present case where $D < 0.01\lambda$, the actual parameters used in the fitting procedure are T_i, T_e/T_i, $[O^+]/N_e$, $[He^+]/([He^+]+[H^+])$ and the normalization factor of the ACF (number densities are indicated by [ ]). Of these parameters, T_i, $[O^+]/N_e$ and the normalization factor are always treated as unknowns. The remaining two are strongly correlated and at least one is normally 'frozen' (HAGEN and HSU, 1974), i.e.

(i) $$T_e/T_i = 1,$$

or

(ii) $$[He^+] = 0.$$

The former assumption leads to the night-time estimation of $T_e(=T_i)$ and the relative concentrations of O^+, He^+ and H^+ ions. This assumption will be practically valid, since the magnitude of the difference between T_i and T_e is relatively small below 500 km, although perceptible thermal non-equilibrium is evident at the higher altitudes (PRASAD, 1970). The latter assumption gives the daytime estimates of T_e and T_i as well as the relative concentrations of O^+ and H^+ ions. The assumption which gives the smaller square error in the fitting is used near sunrise and sunset and near *conjugate* sunrise and sunset in the northern hemisphere winter.

Electron densities are determined from the measured power profile (e.g. EVANS, 1969). The value determined is corrected for T_e/T_i and Debye length (MOORCROFT, 1964), and normalized to the F2-region peak electron density as determined by an on-site ionosonde.

2.3 *Averaging*

Table 1 lists the dates and times for which measurements were successfully carried out and analyzed. Included in the table is the 3 h average of planetary magnetic index K_p in each period of observation. Of the 19 nights observed, three nights belong to summer (May–July), six nights to autumn (August–October), nine nights to winter (November–January), and the remaining one night to spring (February–April). In the following the mean nocturnal variation of ionospheric parameters will be derived for summer, autumn and winter conditions, with the one night in spring included in the autumnal variation. This represents a convenient way of organizing a limited amount of data in which a clear summer/winter difference is evident.

There is appreciable difference in the absolute values of the ionospheric parameters observed on individual days, depending largely on season and solar and geomagnetic activities (MOORCROFT, 1969; PRASAD, 1970), so that the simple averaging uniformly weighted might emphasize the contribution from the days of special conditions, for example, of high solar or geomagnetic activities when electron density or temperatures are considered. Therefore we average the parameter for all nights belonging to the same season in a way described below. First, an ionospheric parameter $x_i(t_j)$ obtained at time t_j on the ith night is normalized by the average,

$$\bar{x}_i = \frac{\sum_{j=1}^{M_i} x_i(t_j)}{M_i}, \tag{1}$$

where M_i is the total number of observations for the ith night. The normalized values $x_i(t_j)/\bar{x}_i$ are then averaged over N nights to obtain a mean nocturnal value for each season, i.e.

$$\bar{x}(t_j) = \frac{\sum_{i=1}^{N} \bar{x}_i}{N^2} \sum_{i=1}^{N} \frac{x_i(t_j)}{\bar{x}_i}. \tag{2}$$

The observation times differ every night, and all data are rearranged by linear interpolation to the values at 0, 15, 30 and 45 min for every hour. A three-point running average is made over the time sequence of the mean values to discriminate rotational effects of the antenna beam direction, giving the time resolution of about one hour for all quantities except the ion drift velocity (~1.5 h).

3. RESULTS FOR THE MEAN STRUCTURE

3.1 *Ion and electron temperatures*

Figures 1(a)–(c) are diagrams for summer, autumn and winter, respectively, showing the mean

Table 1. Dates, AST times, and 3 h K_p for the observations used in this report

Date	Time(LT)	K_p (3 h average) 1200–1500	1500–1800	1800–2100	2100–0000	0000–0300	0300–0600	0600–0900	0900–1200 LT
17–18 Sept. 1974	1902–618	1	1–	0	0	0	1–	2+	1–
18–19	1828–614	5–	6–	3–	3+	6–	3+	5+	5–
31 Oct.–1 Nov.	1940–707	0+	2–	3–	2+	3–	2+	1	1–
7– 8	1941–714	1	2+	2+	1	2+	2–	1+	1
8– 9	1930–541	3	3	5	6–	5+	6–	6–	5–
9–10	1946–730	5–	4	2	2+	2+	3	2+	1
12–13	1831–603	6–	5+	6–	5+	5–	4	4+	5–
5– 6 Jan. 1975	1948–836	4	4+	4+	4+	3	2+	2	2+
15–16	1833–736	4–	4+	3+	4+	4	3+	5	4+
15–16 Apr.	1855–535	2–	3–	2+	2–	3–	2+	2+	1
18–19 May.	1848–609	2–	2	2	2+	3	3	3–	2
10–11 June	1915–545	1	1+	1	1+	2	2–	3+	4+
15–16 July	1704–555	4–	3+	3–	2+	3+	3	2+	3
12–13 Sept.	1759–437	4	2+	2–	2+	4	4+	2+	4+
14–15 Oct.	1837–630	2+	3–	2	2+	1	2–	1+	2+
19–20	1825–736	1	1	2–	1+	2–	1+	1–	1–
13–14 Dec.	1739–633	0+	2–	1	1	1	0+	1	1
27	1800–2331	3–	5+	5	4–	4+	3+	3	2
20–21 Jan. 1976	1819–629	2–	3+	2+	3+	3+	4	3+	4–

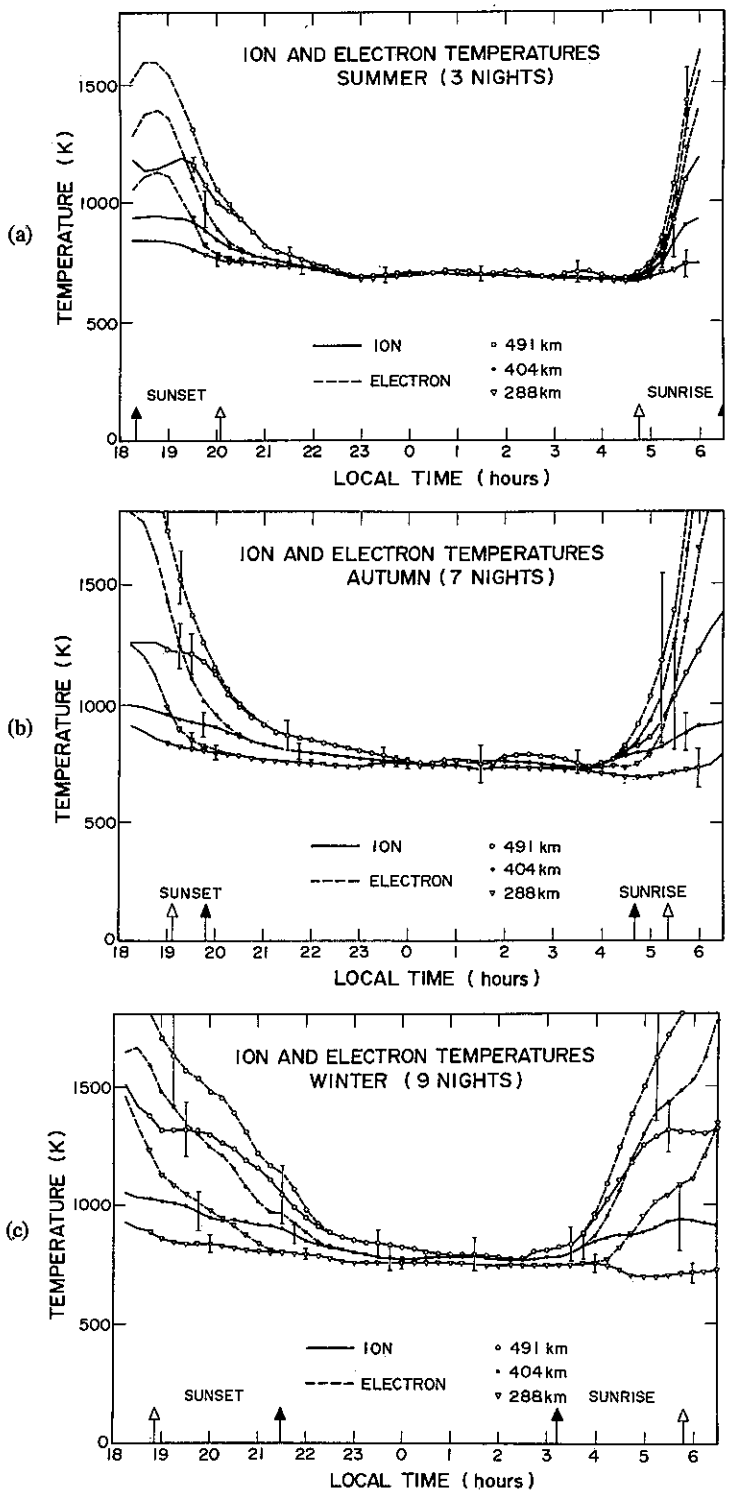

Fig. 1. Night-time variation of the mean ion (solid lines) and electron (broken lines) temperatures at 288, 404 and 491 km for (a) summer, (b) autumn and (c) winter. No symbol is put to the lines if the number of data available is less than three in summer and five in other seasons.

night-time variation of ion and electron temperatures at three altitudes separated by almost 100 km. The vertical lines in these figures and some of the following figures are the error bars that represent the standard deviations of the individual-day values about the mean value. The upward arrows at the bottom indicate the times of sunset and sunrise at the altitude of 400 km at Arecibo and its conjugate point. The times were estimated as the moments when the sun appears above and disappears below the screen height of 200 km, using the computer code of COLIN and MYERS (1966).

In summer it requires less than one hour after sunset before attaining thermal equilibrium whereas more than three hours are necessary in winter due to conjugate photoelectron heating (CARLSON, 1968). Conjugate photoelectron heating is also evident two hours before sunrise in winter when a rapid increase in the electron temperature (pre-local winter sunrise enhancement) is observed. The ion (or electron) temperature near summer midnight is almost constant over the height range considered; however, there seems to be a slight height gradient of the temperature in winter (PRASAD, 1968).

The midnight mean temperature is 700 K in summer and around 770 K in autumn and winter. The temperature remains almost constant for more than several hours around midnight. This flatness is not observed in the JACCHIA (1971) model that changes, in essence, sinusoidally, and is possibly due to the semidiurnal tidal oscillation that is important at low latitudes (GARRETT and FORBES, 1978; HARPER, 1979).

3.2 *Electron density*

Electron densities at heights near the *F*2-peak are shown vs time in Fig. 2. The variation at 259 km is also included in the same figure for comparison. Exponential decays are seen in all seasons, although the decay rate differs with season. The rate is steepest in summer, whereas it seems extremely small in winter, as generally observed during periods of low solar activity (YONEZAWA, 1965). The *F*2-region peak density tends to increase slightly near midnight. This increase appears as a small hump around 0100 LT in winter, whereas it occurs as a pause on the dominating exponential decay at 2200–0100 LT in summer. This behavior is possibly related to the semidiurnal tide (HARPER, 1979). The variation of electron densities near sunrise, especially at the *F*2-peak, changes with season. In summer the exponential decay of the *F*2-peak electron density

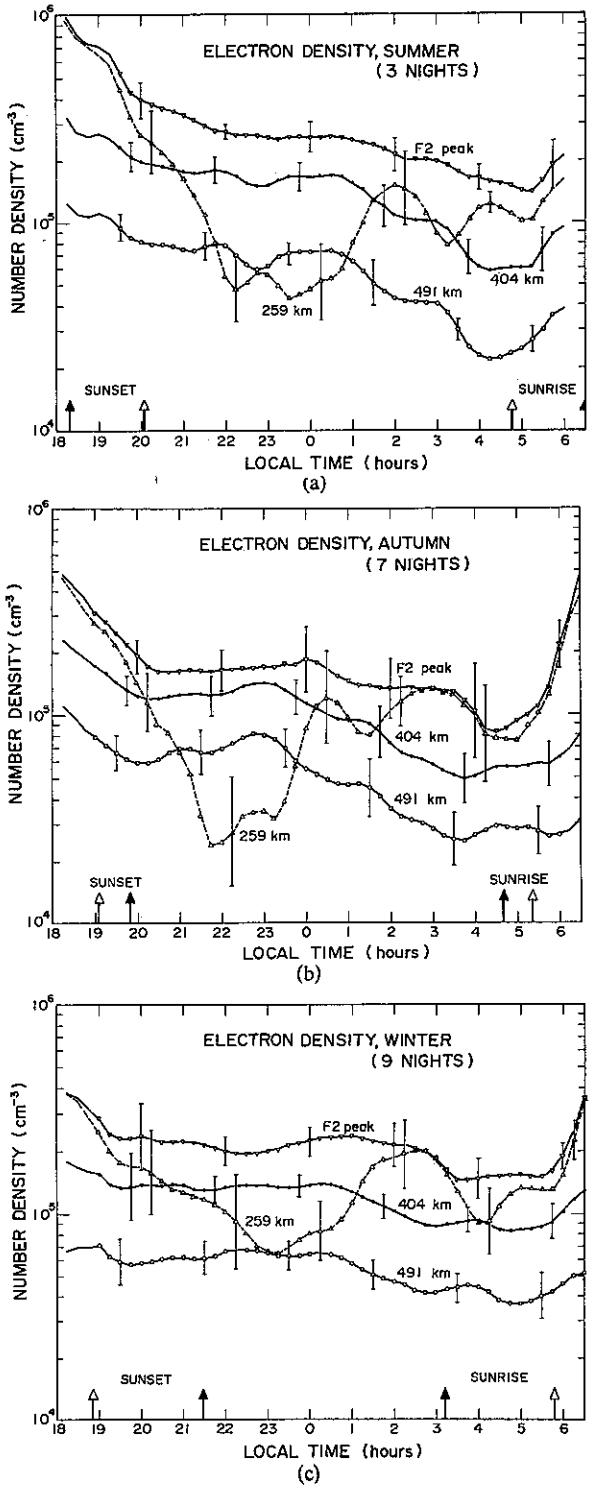

Fig. 2. Night-time variation of the mean electron density at the *F*2-peak and the adjacent altitudes for (a) summer, (b) autumn and (c) winter.

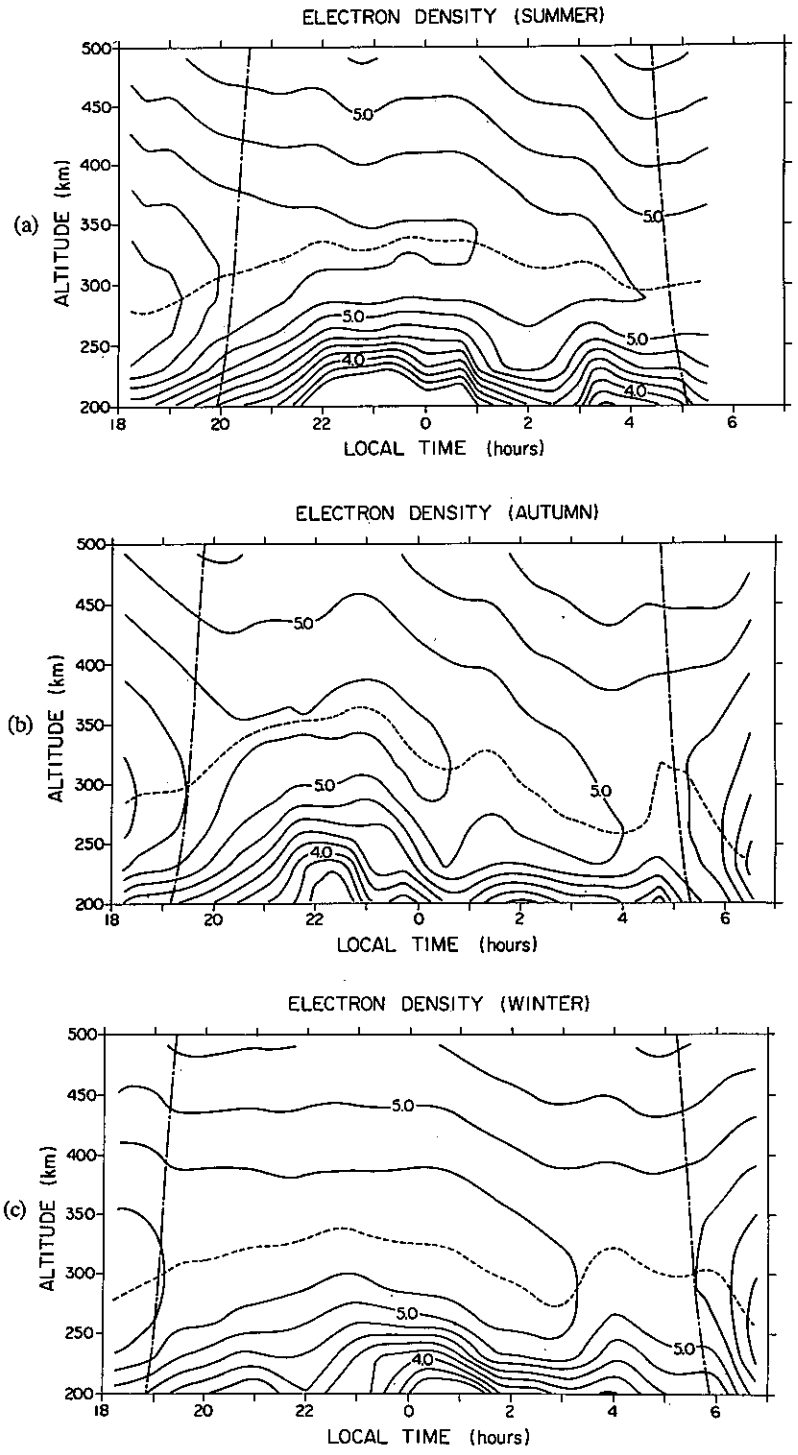

Fig. 3. Contour diagrams of the logarithm of the electron density vs altitude and time for (a) summer, (b) autumn and (c) winter. Broken line and chains indicate respectively the altitude of maximum electron density and the times of the local sunset and sunrise.

continues even after sunrise; however, it ceases two hours before sunrise in winter, with the electron density almost constant until sunrise.

3.3 *Altitude of the F-peak*

Contour diagrams of $\log_{10}(N_e)$ vs. height and time are shown in Figs. 3(a)–(c) for summer, autumn and winter, respectively. The contours are drawn at intervals of 0.2. The figure contains also the $F2$-peak height, $h_{max}F2$, indicated by the broken line. In general, the $F2$-peak observed ascends after sunset and begins to descend near midnight; this type of variation was shown by NELSON and COGGER (1971) to be typical of Arecibo.

Figures 4(a)–(c) show the night-time variations of the altitude of the $F2$-peak and of those levels in the upper and lower regions where the electron density is reduced to one half of that of the $F2$-peak. The thickness of $F2$-layer defined by the height difference of these upper and lower levels of half electron density is roughly proportional to the height of the $F2$-peak above about 165 km, i.e. the base of the F-layer. In addition the altitude of the $F2$-peak increases before sunrise, especially in winter and autumn (NELSON and COGGER, 1971; BEHNKE and HARPER, 1973). The time of the ascent is almost coincident with that when the electron temperature starts to increase and the electron density ceases to decrease (CARLSON and WALKER, 1972).

3.4 *Ion drift velocity*

Figures 5(a)–(c) show the vertical component of the ion drift velocity vs. time for three altitudes: 491, 404 and 288 km for the respective seasons. These velocities have been corrected for a transmitter frequency offset of $7\,m\,s^{-1}$. There is a strong seasonal difference in the magnitude of the vertical velocities, i.e. the night-time mean is nearly zero in summer, but -20 to $-30\,m\,s^{-1}$ in winter. This seasonal difference seems qualitatively consistent with the decay rates of electron density, which are steepest in summer and relatively small in winter.

The vertical velocity has a local time variation. In autumn and winter the vertical ion velocities tend to be strongly downwards near sunset, then become relatively small in the pre-midnight sector, then strongly downwards again after midnight until about 0400 h. In summer the velocities tend to be weakly downwards near sunset and after midnight, and upwards in the pre-midnight sector.

The seasonal variation of the ion drifts is consistent with the existence of a prevailing wind toward the winter hemisphere at F-region heights, while the local time variation of V_z is probably due to the effects of diurnal and semidiurnal winds of comparable amplitude at F-region heights (HARPER, 1979).

Figures 6(a) and (b) give, respectively, the horizontal drift component in the meridional plane and the vertical velocity averaged over the 2000–0400 LT period vs height. The mean meridional drift is northward in all seasons, but much larger in winter than in summer. It is not possible to measure the ion velocity at all local times below 290 km as the electron density becomes very small when the F-layer is high, as is usually the case in the pre-midnight sector. Thus the 'mean' velocities below 290 km emphasize those times when N_e is large, which are the times of large downward V_z. However, it is not understood why the mean meridional velocity remains small at these times.

Figure 6(c) shows the local time variation of the electric field components perpendicular to **B** averaged both over height and season. A significant local time variation is observed in the southward electric field component (eastward ion drifts), the field being southward before midnight and northward after midnight, with an amplitude of 1 to $2\,mV\,m^{-1}$. However, the eastward electric field (upward and northward drift perpendicular to **B**) is very nearly zero at all local times in the averaged data. No significant deviation from this pattern is observed in any season.

The east–west electric fields, of the order of $1\,mV\,m^{-1}$, certainly exist on any given night, with the motion perpendicular to **B** in the meridional plane tending to be in the opposite vertical sense from the motion along **B** (BEHNKE and HARPER, 1973). Thus these fields appear to average out in the mean data.

The source of the electric fields is not clear. If it is principally F-region polarization, one would expect mean southward ion drifts while the F-layer is high, and neutral winds equatorward in the pre-midnight sector. This is not observed. However, if the electric fields are set up by dynamo currents flowing the E-region, one has to explain why a well defined southward electric field variation exists, but the mean eastward electric field is very small. WALKER (private communication, 1978) has shown that the east–west current is zero near heights where layers of enhanced density, which contain the bulk of the conductivity, form in the E-region. However, considerable work remains in elucidating the source or sources of night-time electric fields.

There is a mean vertical gradient in the vertical velocity, $\partial V_z/\partial z$, of the order of $-5\times10^{-5}\,s^{-1}$ over

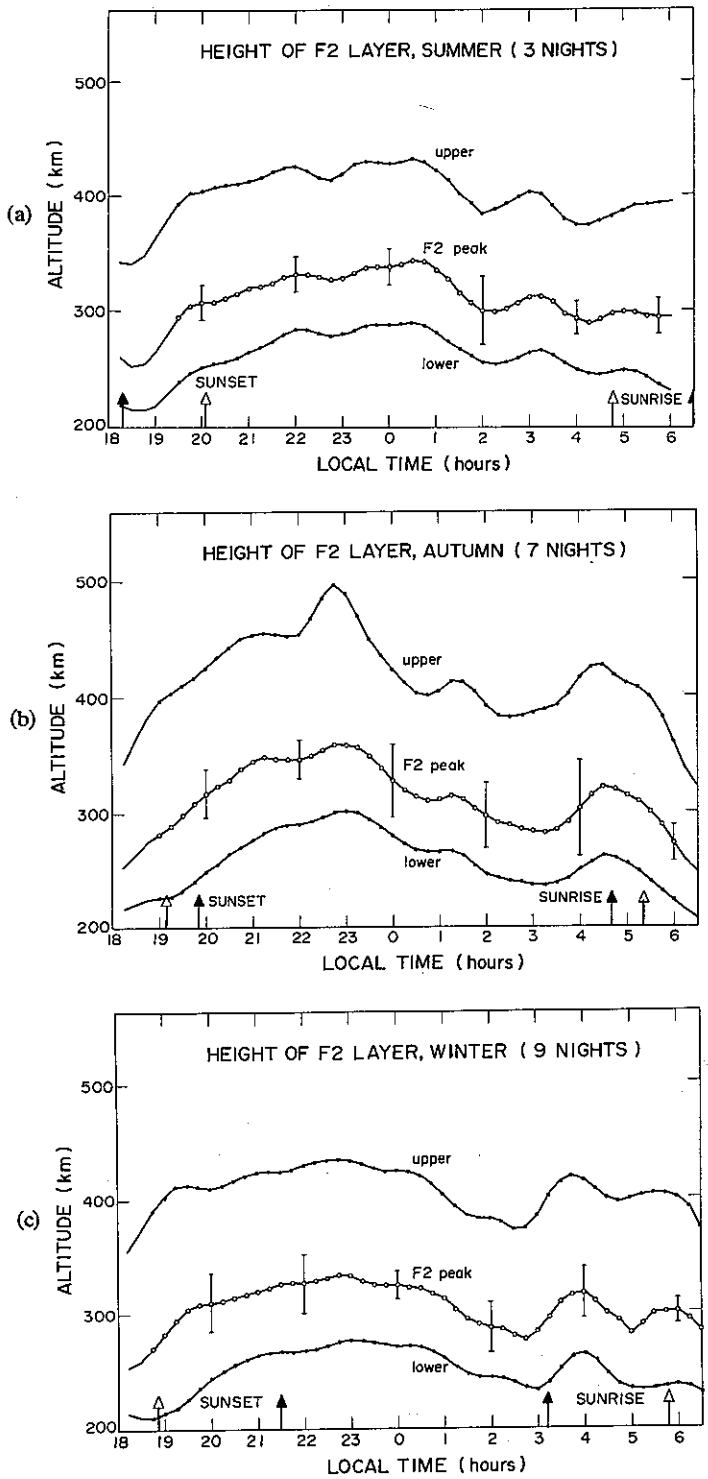

Fig. 4. Night-time variation of the mean altitude of the *F*2-peak for (a) summer, (b) autumn and (c) winter. The adjacent two altitudes where the electron density is reduced to the half of that of the *F*2-peak are also shown.

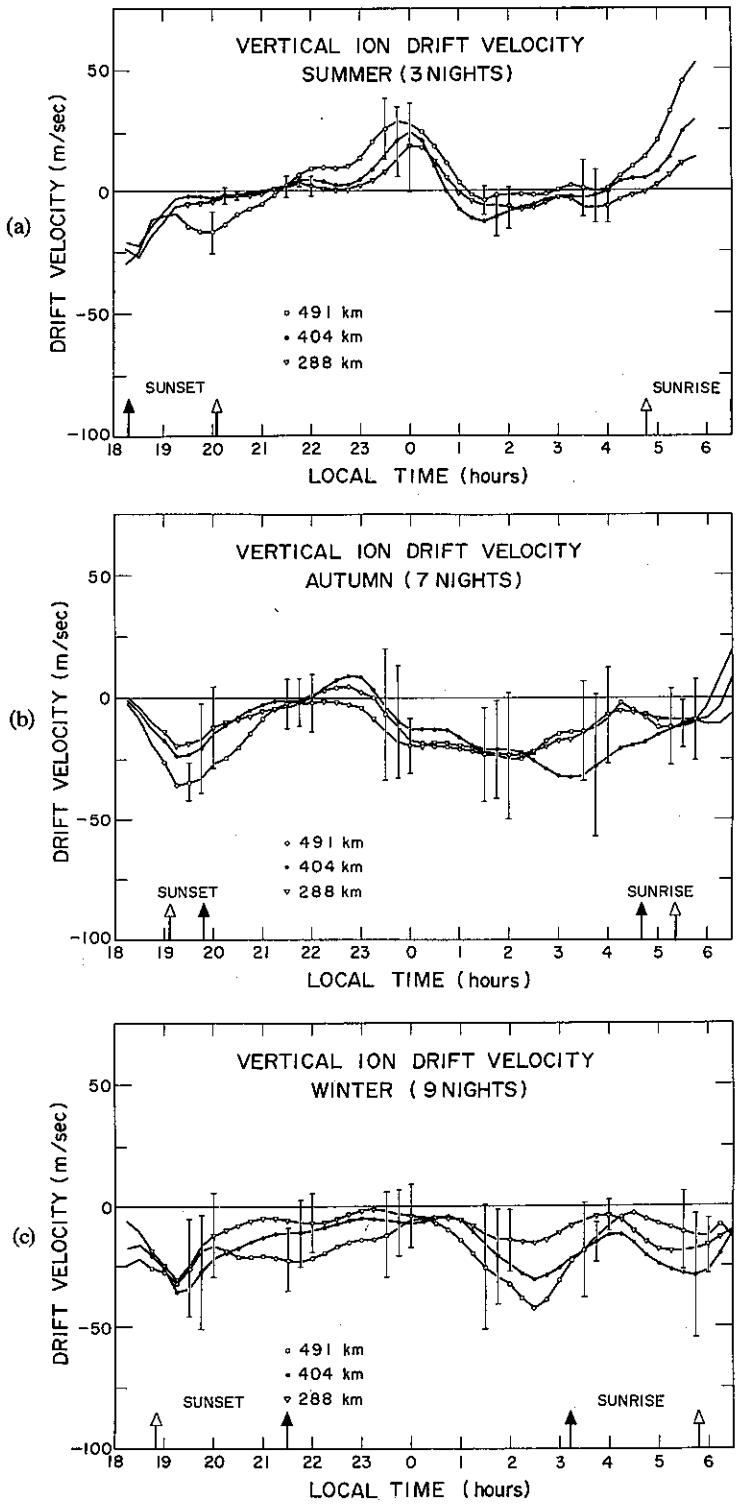

Fig. 5. Night-time variation of the vertical ion drift velocity (upward positive) at 288, 404 and 491 km for (a) summer, (b) autumn and (c) winter.

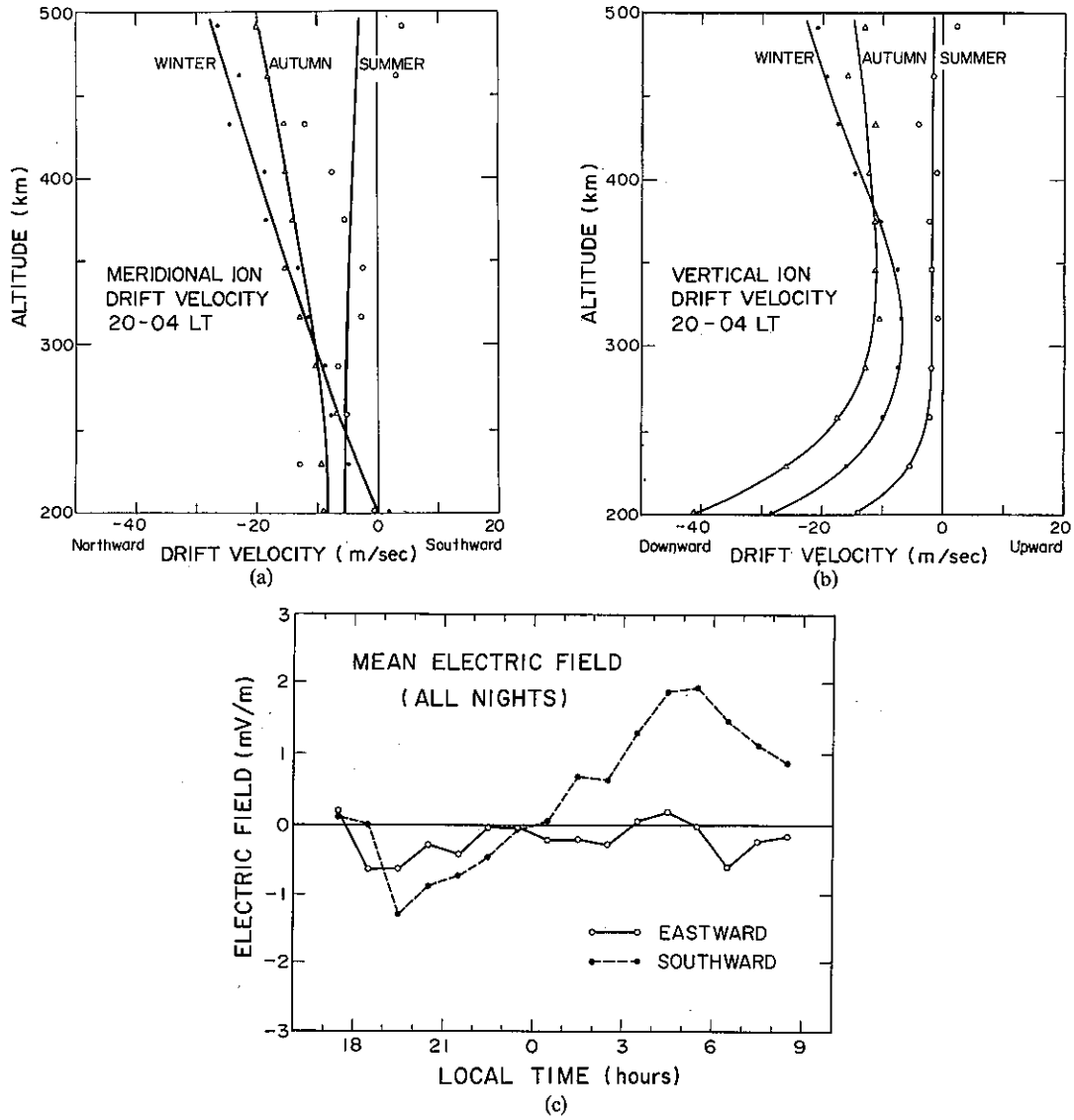

Fig. 6. Seasonal means of (a) meridional (southward positive) and (b) vertical (upward positive) components of ion drift velocity averaged over the period 2000–0400 LT, and (c) night-time variation of the electric field components perpendicular to **B** averaged both over height and season.

the 300–500 km region in autumn and winter. No measurable gradient is observed in summer. It is difficult to infer vertical gradients from the night-time data below 300 km. However, HARPER (1979) has shown that gradients of the order of $\pm 2 \times 10^{-4}$ s^{-1} are associated with the semidiurnal winds over the 200–300 km region from daytime measurements. These vertical gradients in V_z appear to be principally responsible for the postmidnight increases in the $F2$-peak electron density, N_{max}, that are frequently observed at Arecibo.

3.5 *Light ion composition*

Oxygen ions predominate during daytime in the topside ionosphere over Arecibo, with a larger abundance of light ions found at night (MOORCROFT, 1969; PRASAD, 1968, 1970; HO and MOORCROFT, 1971, 1975; HAGEN and HSU, 1974). Figures 7(a)–(c) illustrate the mean night-time variation of H^+ ion at the four uppermost altitudes. It is obvious in the figures that there is an appreciable fraction of H^+ ion present at night at altitudes as

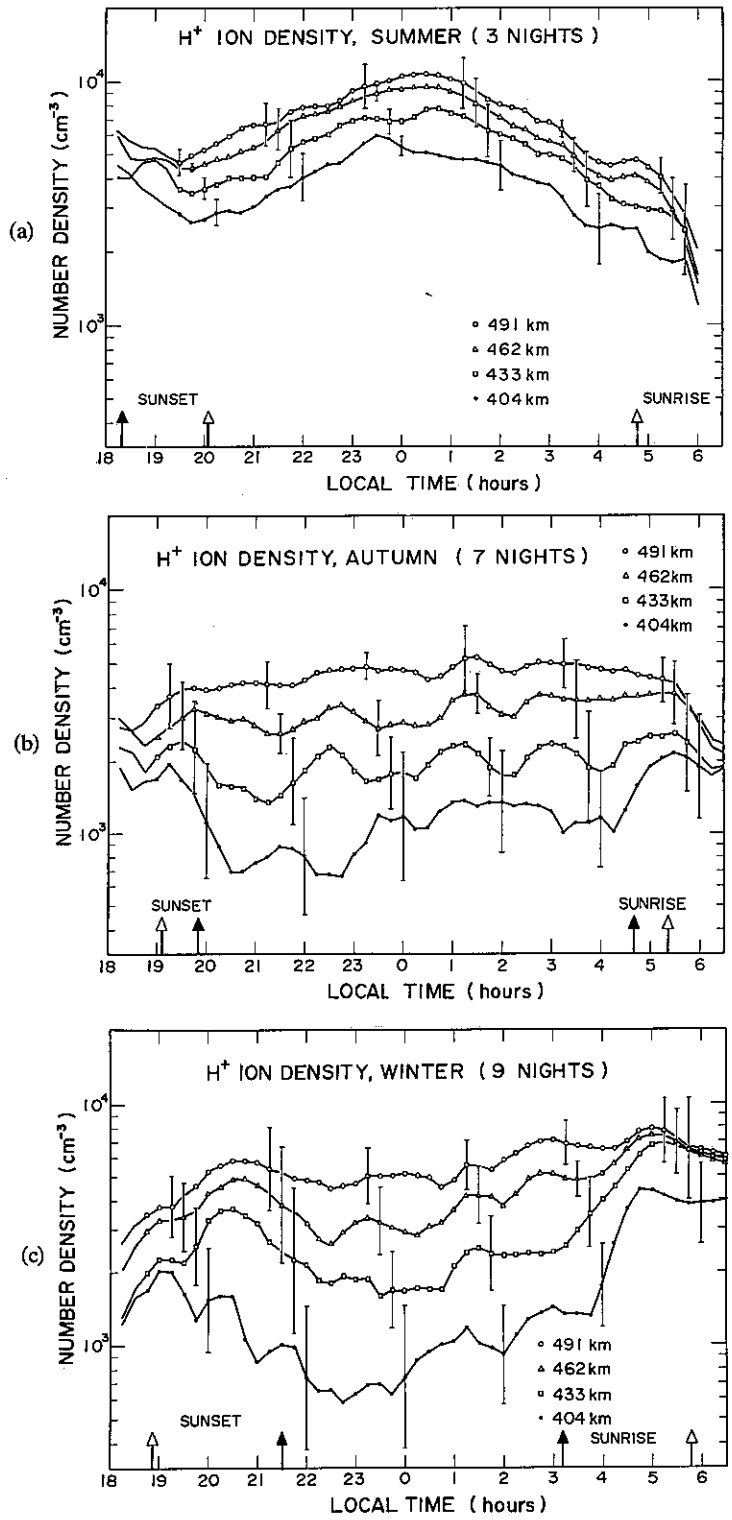

Fig. 7. Night-time H^+ ion concentration variation at various altitudes above 400 km for (a) summer, (b) autumn and (c) winter.

low as 400 km. The variation of the H^+ ion concentration as a function of time shows a marked seasonal difference. The concentration is maximized near midnight in summer, whereas it is considerably increased near sunrise and sunset in winter. The maximum concentration at about 500 km reaches more than 10^4 and 8×10^3 cm^{-3} in summer and winter, respectively.

The maximum value of the relative concentration of the H^+ ion to the electron density at 500 km ranges from 20% to 70% depending upon season and geomagnetic activity. The mean night-time relative concentration is considerably larger in winter than in summer and sometimes exceeds 50% before sunrise in winter. The O^+/H^+ transition height generally lies no higher than 500 km in winter during the period of present investigation, whereas it increases beyond the observed range in summer. This agrees with the results of MOORCROFT (1969) and PRASAD (1970) from the analyses of the data obtained during the former sunspot minimum years. This low transition altitude is also consistent with recent satellite observations (e.g. TAYLOR, 1971; TITHERIDGE, 1976).

The He^+ ion is found to be a minor constituent and its concentration is relatively small (less than 10%) at all altitudes considered. The abundance ratio of H^+ to He^+ ion observed ranges, in general, from 2 to 7. The H^+ ion predominance over the He^+ ion was shown also during the former sunspot minimum years 1964–1965 (TAYLOR *et al.*, 1970).

4. DISCUSSIONS

4.1 *Solar and geomagnetic dependence*

Figure 8 shows the observed ion temperature averaged over the altitude range 300–500 km and over the period 2300–0300 LT vs the day of obervation. Included in the figure is the exospheric temperature at 0100 LT obtained from the JACCHIA (1971) model. The day-to-day variation of the observed mean temperature is well correlated with that of JACCHIA's model; however, the observed is always higher than the model by about 40 K. Global night-time minimum temperatures T_{min} derived by subtracting the variations with geomagnetic activity, season and latitude from the observed temperatures, through the use of the equations of the JACCHIA (1971) model, are presented for the smoothed 10.7 cm solar flux $\bar{F}_{10.7}$ in Fig. 9. The straight line which is determined by a least squares fit to the derived minimum temperatures is represented by the equation

$$T_{min} = 360 + 3.78\,\bar{F}_{10.7}. \qquad (3)$$

It is clear that the present result is by 20–30 K higher than the JACCHIA model for the observed range of $\bar{F}_{10.7}$. The difference is larger for larger values of $\bar{F}_{10.7}$.

A corresponding geomagnetic activity dependence is observed in the variation of the H^+ ion concentration vs the day of observation. Figure 10 shows the H^+ ion concentration obtained at

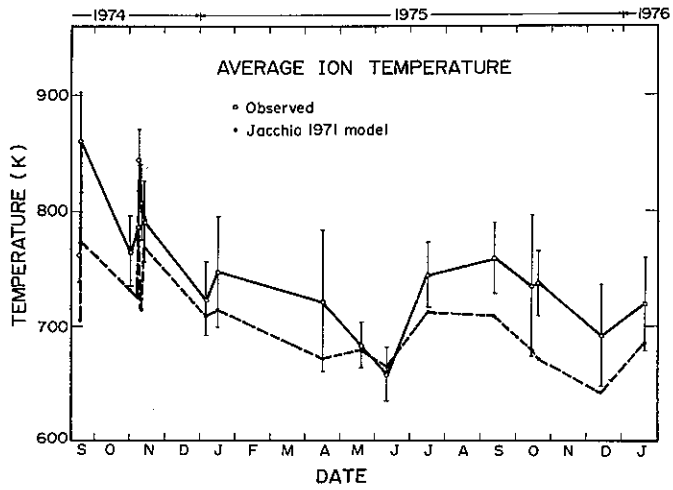

Fig. 8. Observed ion temperature (solid line) averaged over the altitude range 300–500 km and over the period 2300–0300 LT together with the exospheric temperature (broken line) of the JACCHIA (1971) model at 0100 LT.

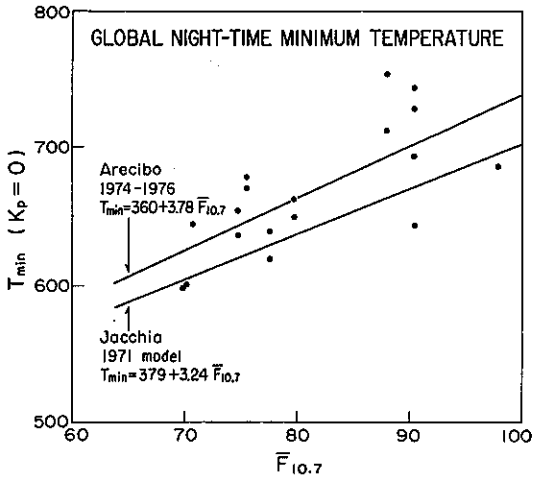

Fig. 9. Global night-time minimum temperatures T_{min} derived, through the use of the equations of the JACCHIA model, from the present observation at Arecibo plotted against $\bar{F}_{10.7}$. The straight line through the observed values is represented by the equation

$$T_{min} = 360 + 3.78\,\bar{F}_{10.7},$$

whereas that of the JACCHIA (1971) model is

$$T_{min} = 379 + 3.24\,\bar{F}_{10.7}.$$

0000 LT at the altitude of 491 km and the 24 h summation of the K_ps centered at 0000 LT. A negative correlation is apparent between them. The small increase of the H^+ ion concentration seems to be present in response to the slight decay of the solar activity during the period of observation 1974–1976; however, more data must be analyzed before the extent of the solar and geomagnetic differences can be clearly established. The H^+ ion concentration below the O^+/H^+ transition height decreases when the transition height is raised by the expansion of the *F*2-region under active geomagnetic conditions (e.g. BATES and PATTERSON, 1961). Millstone Hill observations have also revealed that the largest H^+ relative concentrations are usually encountered when the exospheric temperature is low (EVANS, 1975).

4.2 *Maintenance of the night-time ionosphere*

It is widely believed that the night-time *F*2-region is maintained by the inflow of the ionization which escaped to the protonosphere during the daytime (e.g. YONEZAWA, 1965; PARK and BANKS, 1974). However, recent incoherent scatter observations at high geomagnetic latitude stations have estimated arriving fluxes which are insufficient to maintain the night-time *F*2-region (EVANS, 1975; JAIN and WILLIAMS, 1974), whereas an observation at Arecibo indicated sufficient downward fluxes during night-time (HAGEN and HSU, 1974).

In this section we will discuss whether the ionospheric quantities observed at Arecibo satisfy the continuity of ionization. The following discussion assumes *a priori* that there are neither horizontal gradients of the ionosphere nor horizontal plasma motions, although a comparison of Figs. 3(a)–(c) and 6(a)–(c) shows that this is not the case. However, the discussion will lead to a result which

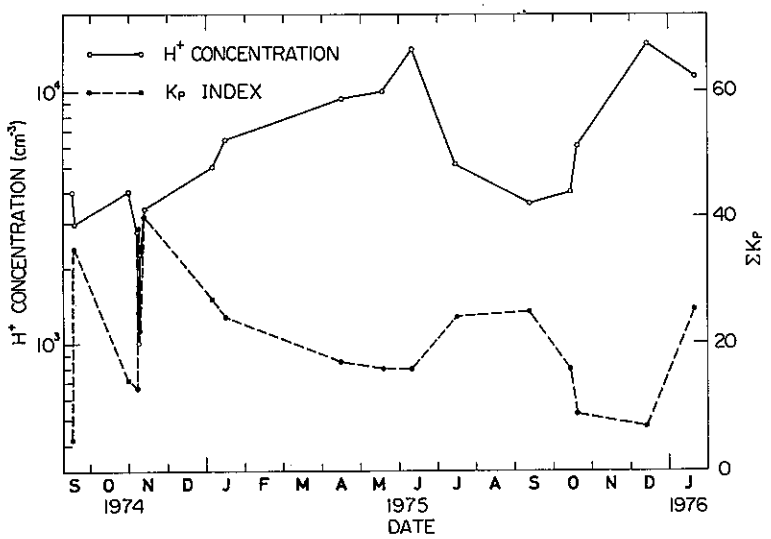

Fig. 10. H^+ ion concentration (solid line) observed at 0000 LT at the altitude of 491 km and the 24 h summation of the K_ps centered at 0000 LT (broken line).

indicates that both the horizontal gradients in electron density and horizontal plasma velocities are, on average, not the major contributor maintaining the night-time $F2$-region at Arecibo. The continuity equation is

$$\frac{\partial N_e}{\partial t} = q - \beta N_e - \mathrm{div}\,(N_e \mathbf{V}), \tag{4}$$

where N_e is the electron density, q the ionization production rate, β the attachment coefficient and $\mathbf{V}$ the ion drift velocity. Assuming that $q = 0$,

$$\beta = -\frac{1}{N_e}\left[\frac{\partial N_e}{\partial t} + \frac{\partial}{\partial z}(N_e V_z)\right], \tag{5}$$

where V_z is the vertical component of the ion drift velocity. Equation (5) may give βs vs. altitude for the region under consideration by adapting the estimates obtained in the preceding chapter to the quantities on the RHS. However, the variation of β as a function of altitude thus calculated does not show the exponential decay that is widely accepted (PARK and BANKS, 1974), rather the coefficient is appreciably enhanced above the $F2$-peak.

Instead the virtual production rate Q which is necessary to fulfill the equation of continuity,

$$Q = \frac{\partial N_e}{\partial t} + \beta N_e + \frac{\partial}{\partial z}(N_e V_z), \tag{6}$$

will be derived by using the theoretical value of β (PARK and BANKS, 1974) given by

$$\beta = \frac{1.1\times 10^9}{T_i^{0.7}}[O_2] + \left[12 - \frac{T_n - 300}{50} + \frac{(T_n - 300)(T_n - 600)}{3.5\times 10^4}\right]\times 10^{-13}[N_2]\,[s^{-1}]. \tag{7}$$

Thermal equilibrium is assumed so that the ion temperature observed (T_i) may be adapted also for the neutral temperature (T_n). The number densities of O_2 and N_2, $[O_2]$ and $[N_2]$, are taken from the JACCHIA (1971) model. Figure 11 shows Q averaged over the period 2200–0400 LT. The error bars indicate the values of the rms deviations of Qs derived on individual days of observation. The values of Q are, in general, positive in the altitude range around 300 km, whereas they are negative around 400 km.

A systematic error is encountered in the determination of the line-of-sight drift velocity due to a change in the transmitter frequency during the transmitted pulse (transmitter chirp). It was not possible to measure the offset during the observations. An offset of approximately 13 m s^{-1} has been estimated from other test measurements at Arecibo (HARPER *et al.*, 1976), whereas offsets of the order of 10 m s^{-1} have been reported by EVANS (1975) at Millstone Hill. The same order of velocity offset was probably encountered in the present observation. The offset (ϵ) in the line-of-sight velocities affects the vertical velocity component by $\epsilon/\cos 15° = 1.04\epsilon$ m s^{-1}, since the antenna is tilted 15°

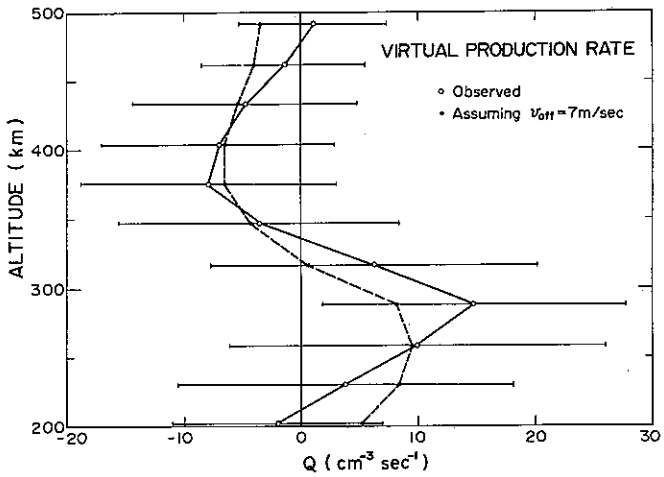

Fig. 11. Virtual production rate (solid line) which is necessary to fulfill the equation of continuity and the virtual production rate due to the offset of 7 m s^{-1} in the observed vertical velocity. Both are the average over the period 2000–0400 LT. The horizontal lines show the rms deviations of the estimates on individual days of observation.

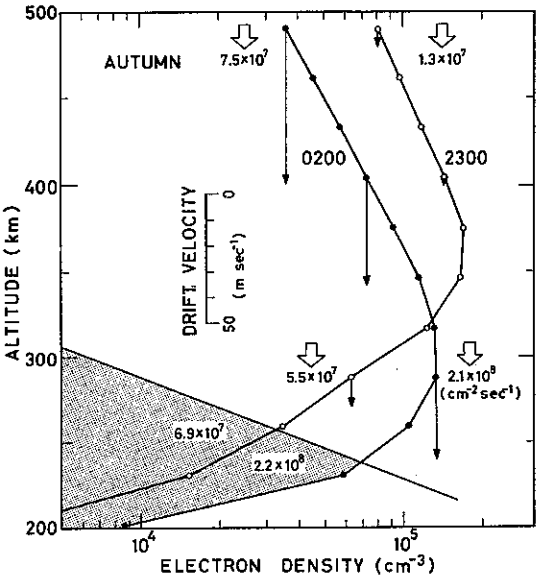

Fig. 12. Electron density (solid lines) vs altitude and vertical component of ion drift velocity (thin arrows) observed at the altitudes of the root of arrow at 2300 and 0200 LT in autumn. Thick arrows indicate the downward fluxes of ionization which pass a unit area per second at 300 and 500 km. The numbers put in the shaded region are the amounts of ionization which is recombined per second in a column with unit cross-section.

from the zenith in our case. Hereafter we designate the vertical velocity offset as V_{off}. This offset leads to a virtual production rate $V_{off}(\partial N_e/\partial z)$ which is similar to that required for fulfilling the equation of continuity. Figure 11 includes the variation of $V_{off}(\partial N_e/\partial z)$ for an offset of $7\,m\,s^{-1}$, which was found to best fit the averaged data. Although the uncertainty of Qs derived is quite large, the overall agreement between the profiles of Q and $V_{off}(\partial N_e/\partial z)$ is good throughout the region considered. The difference between both profiles does not seem to be markedly larger in the region below 250 km where appreciably large downward velocities are observed. The vertical components of the ion velocity, when corrected by the offset velocity, seem to satisfy the equation of continuity without such *ad hoc* ionization and the horizontal inhomogeneity of the ionosphere likely to be necessary at Millstone Hill (Evans, 1975) and at Malvern (Jain and Williams, 1974). Therefore, the night-time variation of the electron density may consistently be described only in terms of the downward flux of ionization at Arecibo during the period of the present observation. The difference may be due to the latitudinal difference between Arecibo (Geomagnetic Latitude 30°N) and Millstone Hill (Geomagnetic Latitude 53°N) or Malvern (Geomagnetic Latitude 56°N).

The continuity of ionization is also obtained on shorter time scales. Figure 12 depicts the variations of the electron density as a function of altitude at 2300 LT in autumn when the $F2$-peak is raised up to the highest and at 0200 LT during the period of descent of the peak. The thin arrows indicate the vertical component of ion drift velocity at the respective times, whereas the thick ones show the amount of ionization fluxes which pass through a unit cross-sectional area ($1\,cm^2$) per second at 300 and 500 km. The numbers put in the shaded region below 300 km indicate the amount of ionization which is recombined per second in a column with the unit cross-section. It is apparent from the figure that the magnitudes of the vertical flux at 300 km coincide well with the amounts of recombination below 300 km. The larger velocity of the downward drift at 0200 LT when the $F2$-peak is lowered to the more dissipative range of altitude well compensates the larger dissipation of ionizations there. At 2300 LT when the amount of recombination is relatively small below 300 km the downward drift is extremely small throughout the region observed. It is also shown that the vertical fluxes of ionization are larger at 300 km than at 500 km in these instances. The decay rate of the electron density predicted by this outflow almost coincides with that of the observed electron density.

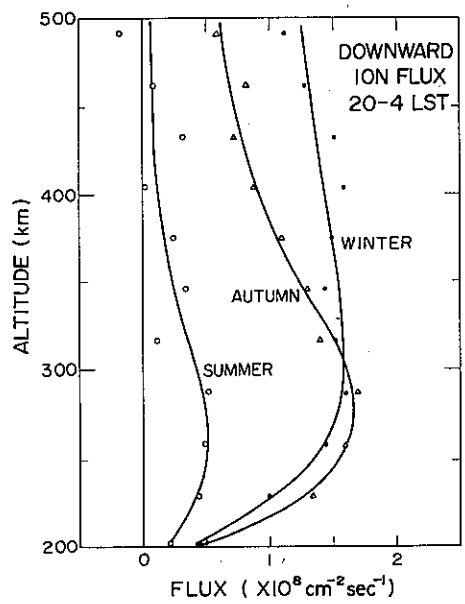

Fig. 13. Variation of the vertical flux of ionization averaged over the period 2000–0400 LT as a function of altitude (downward positive).

Figure 13 shows the profile of the vertical ionization flux averaged over the period 2000–0400 LT for respective season. It is clear from the figure that the flux at night is downward for all seasons over the height range considered. The result seems reliable enough to permit discussion of seasonal trends. The roughly constant flow above 300 km in winter may indicate the presence of a flux of ionization descending to lower altitudes. The flux observed above 500 km is likely to be more than 10^8 electron $cm^{-2} s^{-1}$ in winter, considerably larger than the estimates from higher latitude incoherent scatter measurements (EVANS, 1975; JAIN and WILLIAMS, 1974). The results presented here suggest that the night-time fluxes are the principal means of maintaining the night-time *F*-region in winter over Arecibo, although they are generally small and not the major contributor at Millstone Hill and Malvern.

5. CONCLUSIONS

Seasonal mean variations of ion and electron temperatures, electron density, altitude of the *F*2-peak, ion drift velocity, and concentration of H^+ ions are presented as functions of time and altitude, based on 19 nights of Arecibo data taken during the sunspot minimum years 1974–1976.

Our main conclusions are as follows:

(1) The night-time *F*2-region at Arecibo is principally maintained by a downward flux of ionization. There is a marked seasonal difference in magnitudes of the mean vertical velocities and fluxes, with larger downward values in winter. This seasonal difference is consistent with the decay rates of night-time electron density. The amount of flux in winter seems to be more than 10^8 electron $cm^{-2} s^{-1}$. There is a mean vertical gradient in the vertical velocity, $\partial Vz/\partial z$, of the order of $-5 \times 10^{-5} s^{-1}$ over the 300–500 km region in autumn and winter. No measurable gradient is observed in summer.

(2) The variation of electron density as a function of time is closely related with those of the vertical ion velocity and the altitude of the *F*2-peak. The thickness of the night-time *F*2-layer is roughly proportional to the height of the *F*2-peak above 165 km. The ionization flux and velocity are roughly inversely proportional to altitude of the layer; downward flux and velocity are large, when the layer is low, and vice versa.

(3) The H^+ ion concentration in the *F*2-region shows a marked seasonal difference and the relative concentration of H^+ ion to the electron density at 500 km sometimes exceeds 50% before sunrise. This lower altitude of the O^+/H^+ transition in the latitudes of Arecibo is consistent with recent satellite observations. A strong anti-correlation of the H^+ ion concentration with magnetic activity is observed. The He^+ ion concentration is relatively small (generally less than 10%) at all altitudes below 500 km.

(4) The time and altitude variations of ion temperature are small and the ion temperature remains almost constant for several hours around midnight. This flatness is not observed in the JACCHIA (1971) model. The observed ion temperatures average about 20–30 K higher than the prediction of the JACCHIA (1971) neutral model for the observed range of $\bar{F}_{10.7}$.

Graphed and 15 min tabulated values of the ionospheric parameters described here for individual days are available upon request from Kyoto University (FUKAO *et al.*, 1977).

Acknowledgements—The authors thank Professor T. YONEZAWA, Chubu Technical College, for frequent and stimulating discussions and for his critical reading of the manuscript. They are also grateful to Professor S. KATO, Ionosphere Research Laboratory, for his encouragement throughout this work. Support for this research was provided by the Ministry of Education of Japan under Grant 146034. The work of one of us (RMH) was supported by the U.S. National Science Foundation under Grant ATM 77-20240.

REFERENCES

BATES D. R. and PATTERSON T. N.	1961	*Planet. Space Sci.* **5,** 257.
BEHNKE R. A.	1979	*J. geophys. Res.* **84,** 974.
BEHNKE R. A. and HARPER R. M.	1973	*J. geophys. Res.* **78,** 8222.
CARLSON H.C.	1968	*Radio Sci.* **3,** 668.
CARLSON H.C. and WALKER J. C. G.	1972	*Planet. Space Sci.* **20,** 141.
EVANS J. V.	1969	*Proc. Instn. Elect. Electron. Engrs.* **57,** 496.
EVANS J.V.	1975	*Planet. Space Sci.* **23,** 1611.
GARRETT H. B. and FORBES J. M.	1978	*J. atmos. terr. Phys.* **40,** 657.
HAGEN J. B. and HSU P. Y.-S.	1974	*J. geophys. Res.* **79,** 4269.
HARPER R.M.	1979	*J. geophys. Res.* **84,** 411
HARPER R. M., WAND R. H., ZAMLUTTI C.J. and FARLEY D.T.	1976	*J. geophys. Res.* **81,** 25.
HO M. C. and MOORCROFT D. R.	1971	*Planet. Space Sci.* **19,** 1441.

Ho M. C. and Moorcroft D. R.	1975	*Planet. Space Sci.* **23,** 315.
Ho M. C. and Moorcroft D. R.	1977	*J. atmos. terr. Phys.* **39,** 1317.
Jain A. R. and Williams P. J. S.	1974	*J. atmos. terr. Phys.* **36,** 417.
Moorcroft D. R.	1964	*J. geophys. Res.* **69,** 955.
Moorcroft D. R.	1969	*J. geophys. Res.* **74,** 315.
Nelson G. J. and Cogger L. L.	1971	*J. atmos. terr. Phys.* **33,** 1711.
Park C. G. and Banks P. M.	1974	*J. geophys. Res.* **79,** 4661.
Prasad S. S.	1968	*J. geophys. Res.* **73,** 6795.
Prasad S. S.	1970	*J. geophys. Res.* **75,** 1911.
Rishbeth H. and Garriott O. K.	1969	*Introduction to Ionospheric Physics,* Academic Press, New York.
Taylor H. A. Jr	1971	*Planet. Space Sci.* **19,** 77.
Taylor H. A. Jr, Mayr H. G. and Brinton H.C.	1970	*Space Res.* **X,** 663.
Titheridge J. E.	1976	*Planet. Space Sci.* **24,** 229.
Vickrey J. F., Swartz W. E. and Farley D.T.	1976	*Geophys. Res. Lett.* **3,** 217.
Wand R. H. and Perkins F.W.	1970	*J. atmos. terr. Phys.* **32,** 1921.
Yonezawa T.	1965	*Space Res.* **V,** 49.

Reference is also made to the following unpublished material:

Colin L. and Myers M. A.	1966	Computed times of sunrise and sunset in the ionosphere, *TM X-1233,* NASA Ames Research Center, Moffet Field, Calif.
Fukao S., Sato T., Kimura I. and Harper R. M.	1977	Night-time ionospheric parameters in the 200–500 km region observed by Arecibo incoherent scatter radar during 1974–1976, Kyoto University.
Jacchia L.G.	1971	Revised static models of the thermosphere and exosphere with empirical temperature profiles, *Spec. Rep.* **332,** Smithsonian Astrophys. Obs., Cambridge, Mass.
Waldteufel P.	1971	On the analysis of high altitude incoherent scatter data, **AO 30,** Arecibo Observatory, Puerto Rico.